Theory for tailoring sonic devices: Diffraction dominates over refraction

N. Garcia,[1] M. Nieto-Vesperinas,[2] E. V. Ponizovskaya,[1] and M. Torres[1,*]
[1]*Laboratorio de Física de Sistemas Pequeños y Nanotecnología, Consejo Superior de Investigaciones Cientificas, Serrano 144, 28006 Madrid, Spain*
[2]*Instituto de Ciencia de Materiales de Madrid, Consejo Superior de Investigaciones Científicas, Campus de Cantoblanco, Madrid 28049, Spain*

(Received 26 March 2002; revised manuscript received 18 July 2002; published 15 April 2003)

Acoustic crystal devices, with dimensions on the order of several wavelengths, are studied by using the finite-difference time domain method in the moderately long wavelength propagation regime. *From the focusing and imaging process performed by a square shaped lens, it is shown that diffractive effects dominate over those due to refraction.* The major role of the device edge diffraction is shown by means of the well known Babinet principle. The first examples of imaging with a sonic plane lens, both with crystal structure and massive, and with an acoustic prism able to change the propagation direction of a plane wave, are presented.

DOI: 10.1103/PhysRevE.67.046606 PACS number(s): 43.38.+n, 42.70.Qs, 62.65.+k

New effects of acoustic band gaps [1–3], sound localization and tunneling [4] appear when the wavelength is comparable with the lattice parameter. The moderately long wavelength propagation regime of periodic media (below the first Bragg gap) is of interest, however, and has also been recently utilized to develop appealing and potentially useful photonic [5] and acoustic [6] refractive devices. The refraction effect is based on the fact that wave velocities in the composite and in the surrounding medium are different from each other. It is also claimed that an effective refractive index can be defined in the periodic medium [6]. These refractive properties concern the realm of acoustic and photonic crystal devices. The theory of photonic crystal optics is based on the homogenization of periodic composites [5], which requires structures with a very high number of scatterers (several thousands). These are, in other words, devices with dimensions of several hundred wavelengths. Acoustic periodic composites resembling homogeneous effective media are not realistic, however, due to their required huge size and high internal losses, both for sound and ultrasound propagation. By contrast, the size of realistic sonic devices working in the moderately low frequency region near the gap, such as those recently proposed [6], is of only a few wavelengths. *In such a case, refractive and diffractive effects are intrinsically mixed because the incident wave strongly scatters at the device edges.* In the neighborhood of the gap (where the dispersion is nonlinear), furthermore, isofrequency curves are anisotropically star shaped. This means that the magnitude of the wave vector **k** is not isotropically conserved [7] although the refraction phenomenon relies on the conservation of the component of **k** parallel to the homogenized composite-air interface. This, in turn, implies the appearance of degenerate diffractive indices, i.e., the existence of three different indices for the same frequency; namely, those called: ''phase index'' to describe phenomena related to phase velocity, ''group index'' to account for phenomena related to group velocity, and ''fan index'' that describes phenomena related to beam divergence [7], and constitutes another significantly different mechanism of diffraction within the aforementioned periodic acoustic structures. Therefore, the homogeneous effective medium theory is not appropriate for studying the properties of sonic crystal devices at these rather long wavelengths, and hence an effective refractive index cannot be properly defined. On the other hand, the plane wave (PW) method has been used to study the dispersion relations: frequency ω versus the wave vector **k** in acoustic crystals, where both phase and group wave velocities have been calculated from dispersion relation curves [1,2]. The PW method, however, yields the band structure of waves propagating in infinite periodic systems and its results can only be indirectly compared with wave propagation measurements in a finite system. Reflectance calculations, moreover, are also inevitable to ensure the necessary sonic transparency of devices [6].

To solve these problems, in this paper a finite difference time domain (FDTD) method [8] is used to theoretically study refractive-diffractive sonic composite devices. We show that this allows us to analyze and design finite diffractive elements with dimensions of only a few wavelengths, and to simulate actual experiments in the same way as they are carried out. Alternatively, it is noteworthy that the layer multiple scattering method [9], besides the frequency band structure of an infinite sonic crystal, also provides the transmittance and reflectance of a finite slab of the latter. Our study shows a fact not yet noticed in experiments with this kind of devices: namely, that the images obtained are not only due to refraction mechanisms, but predominantly produced by multiple diffraction effects by the lens surface and inner structure of the periodic composite. As a result, we show that in contrast to conventional optics, imaging formation can be not only obtained with lens-shaped and crystal-like inner structures, but with cubic shapes and massive blocks too. The dominant role of diffraction upon that of refraction in this process of image formation is illustrated by an example based on Babinet's principle of complementary screens.

*Permanent address: Instituto de Física Aplicada, Consejo Superior de Investigaciones Cientificas, Serrano 144, 28006 Madrid, Spain.

We have previously utilized the FDTD method used here, to successfully study elastic band gap materials [3], as well as elastic wave localization phenomena [10]. This method is, furthermore, easily applied to the temporal integration of any acoustic wave propagation equation. We study the propagation of the sonic wave in a structure consisting of parallel and infinitely long cylinders embedded in a host material. The cylinders with radius r are set as either a triangular or a square array with lattice constant a so that different geometries are built. The sonic wave in the composite is given by

$$\frac{\partial^2 u^i}{\partial t^2} = \frac{1}{\rho}\left\{\frac{\partial}{\partial x_i}\left(\lambda \frac{\partial u^l}{\partial x_l}\right) + \frac{\partial}{\partial x_l}\left[\mu\left(\frac{\partial u^i}{\partial x_l} + \frac{\partial u^l}{\partial x_i}\right)\right]\right\}, \qquad (1)$$

where u^i is ith component of the displacement vector $\mathbf{u}(\mathbf{r})$, $\lambda(\mathbf{r})$ and $\mu(\mathbf{r})$ are the Lame coefficients and $\rho(\mathbf{r})$ is the mass density. We assume the propagation in the x-y plane, perpendicular to the cylinders' axis, so the wave equation can be split into two equations [3]

$$\rho \frac{\partial^2 u_x}{\partial t^2} = \frac{\partial T_{xx}}{\partial x} + \frac{\partial T_{xy}}{\partial y}, \qquad (2)$$

$$\rho \frac{\partial^2 u_y}{\partial t^2} = \frac{\partial T_{xy}}{\partial x} + \frac{\partial T_{yy}}{\partial y}, \qquad (3)$$

where $T_{xx} = (\lambda + 2\mu)\partial u_x/\partial x + \lambda \partial u_y/\partial y$, $T_{yy} = (\lambda + 2\mu)\partial u_y/\partial y + \lambda \partial u_x/\partial x$, and $T_{xy} = \mu(\partial u_x/\partial y + \partial u_y/\partial x)$. The longitudinal and the transverse velocities are given by $c_l = \sqrt{(\lambda + 2\mu)/\rho}$ and $c_t = \sqrt{\mu/\rho}$, respectively. Equations (2) and (3) were integrated by means of a FDTD procedure [3,10]. In this scheme, the equations in both the space and the time domains are discretized so that they allow to obtain the actual wave pattern scattered in the composite structure. Furthermore, periodic boundary conditions were set at the boundaries parallel to wave propagation, whereas Mur's first-order absorbing boundary conditions [8] were established at the boundaries perpendicular to the wave propagation direction. To find the reflectance we used a Gaussian pulse. The transmission coefficient was found by normalizing the fast Fourier transform of the part of the initial pulse that passed through the structure, to the fast Fourier transform of the incident pulse. To obtain the distribution of the wave intensity we used the sinusoidal incident wave with a frequency at 1700 Hz, while the intensity was obtained by integrating the value $u_x^2 + u_y^2$ during the wave period. Here we study the case of the aluminum cylinders set in air. FDTD method gives a satisfactory convergence if $dt < [\sqrt{(1/dx)^2 + (1/dy)^2}\, c_l^{\mathrm{Al}}]^{-1}$ [3,10]. The calculations were done with $dx = dy = a/30$ and $dt = 5.89 \times 10^{-3} a/c_l^{\mathrm{Al}}$, $a = 6.35$ cm that gives a good convergence.

A biconvex cylindrical lens made of a triangular periodic arrangement of 32 aluminum cylinders ($c_l = 6400$ m/s and $c_t = 3040$ m/s) in air, illuminated by a plane wave, similar to that of experiment of Ref. [6], has been studied. The corresponding intensity distribution is depicted in Fig. 1(a). The frequency of the incident plane wave is 1700 Hz, and the filling ratio of this numerical experiment is $(\pi/2\sqrt{3})(d/a)^2 = 0.37$, where d is the cylinder diameter and a is the lattice parameter. The numbers near the isophone lines of Fig. 1(a) (boundaries of regions represented in gray scale) are sound wave intensities in decibels. The isophone mapping compares well with that of the experiment of Ref. [6]. From the focal acoustic region to the lowest intensity symmetrical islands, at both sides of the focal region, there is an attenuation of 13.25 dB [Fig. 1(a)], whereas the corresponding experimental value is about 15 dB (Fig. 4 in Ref. [6]). The focal

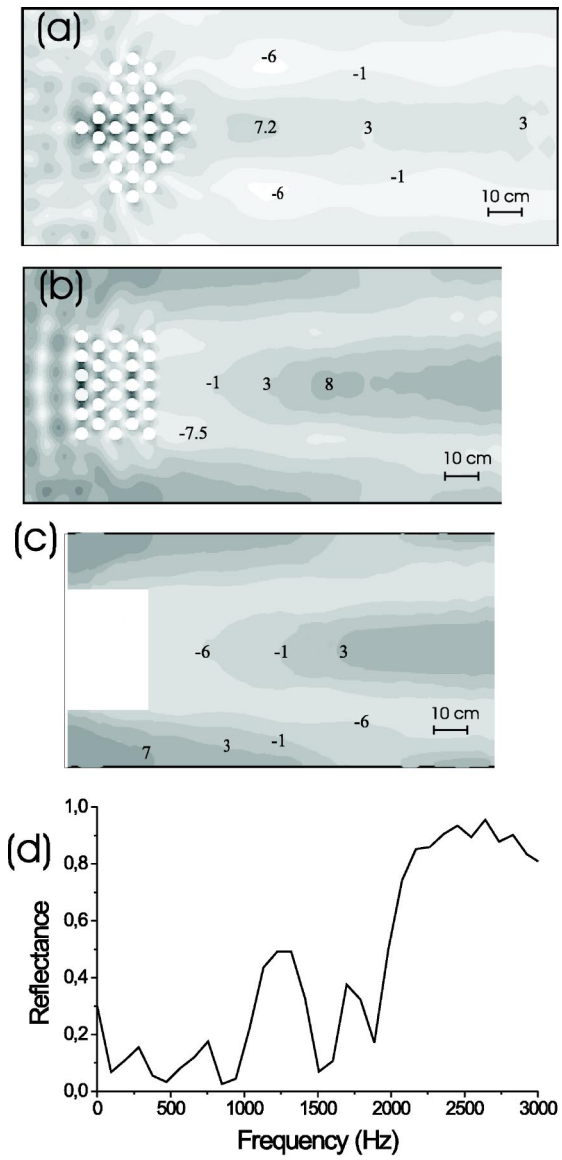

FIG. 1. (a) Intensity pattern of an incident sound plane wave in air, at 1700 Hz, refracted and diffracted by a lenslike periodic arrangement of aluminum rods. An extended focuslike region which is dominated by diffraction can be seen. (b) Intensity pattern of an incident sound plane wave in air, at 1700 Hz, interacting with a periodic squared shape slab of aluminum rods. Notice that the effect of this finite slab is exactly the same as that of (a). (c) Same pattern as in (b) for sound diffracted by a massive aluminum slab. (d) Reflectance spectrum of the finite sonic crystal slab. Bars show the scale in (a), (b), and (c).

length f is defined as the distance from the center of the lens to the point where the maximum intensity is concentrated in Fig. 1(a). For a plane wave impinging from infinity, we obtain $f=41$ cm. Nevertheless, our acoustic lens has an aperture $D=44$ cm which is only twice the wavelength. Its impulse response [12] $[(\lambda\pi)\sin(\pi\Delta x/\lambda f)]/x$ should, therefore, have a width $\Delta x=2f(\lambda/D)$. At 1700 Hz ($\lambda=20$ cm), this should be $\Delta x=37$ cm which agrees perfectly well with the peak width of Fig. 1(a).

In addition, we studied a sonic crystal slab with parallel faces, using the same periodic composite structure and found the same kind of intensity concentration as before [Fig. 1(b)], and even discovered an ''image formation effect'' with a square shaped aluminum block [Fig. 1(c)]. Such unnoticed finding in recent experiments [6] can only be explained by diffraction. The long focal length of this plane lens, shown in Fig. 1(b), was probably unseen in Ref. [6] due to the limited size of the anechoid chamber used. This provides a plausible explanation for the remarkable discrepancy between the present theoretical study and the mentioned experimental report [6]. The FDTD method, moreover, allows us to calculate the reflectance of this finite system, as 1-T, where T is transmittance which is directly calculated by comparing incident and transmitted amplitudes [Fig. 1(d)], and our theoretical calculations fit well with experimental reflectance measurements [6]. As mentioned above, however, our simulated acoustic mapping of the back slab region [Fig. 1(b)] unambiguously exhibits a clear focal zone that is absolutely nonexistent in the corresponding experimental one [6]. There was also a peak in the transmission pattern, due to diffraction, at about 65 cm. In addition, the attenuation from the higher to the lower acoustic intensity regions was 15.5 dB [Fig. 1(b)], even higher than the one generated by the former cylindrical lens with a width of about 33 cm, which is smaller than the expected width of a cylindrical lens of the same focal distance and width ($D=32$ cm), i.e., $\Delta x=80$ cm. This is remarkable, since it suggests that, at sizes comparable to the wavelength as used here, it is possible to focus a wave with a crystal by diffraction effects, which could mimic the refractive effects of a conventional lens.

In order to deeply explore this unexpected acoustic plane lens phenomenon, we present here four imaging numerical experiments (Fig. 2). In Fig. 2(a), a sonic point source is placed at the position O, by introducing at O a time dependent signal with a sharp space distribution of intensity over four cells of the grid, and the corresponding clear acoustic image is generated at location I. We now repeat this theoretical simulation by placing the acoustic point source at the position O, in front of the sonic plane lens [Fig. 2(b)]. Then, a likewise clear image is formed at the point I, as in the former biconvex lens theoretical calculations. In addition, we conducted a third experiment [Fig. 2(c)] with a rectangular piece of aluminum. Interestingly, this latter experiment yields a result similar to those corresponding to Figs. 2(a) and 2(b). It is therefore obvious that the geometrical laws of refraction are not acting between object and image in these structures, what reveals the nonrefractive nature of this phenomenon. Finally, we excite the structure with two point sources O and O' as shown in Fig. 2(d). Then, two mutually

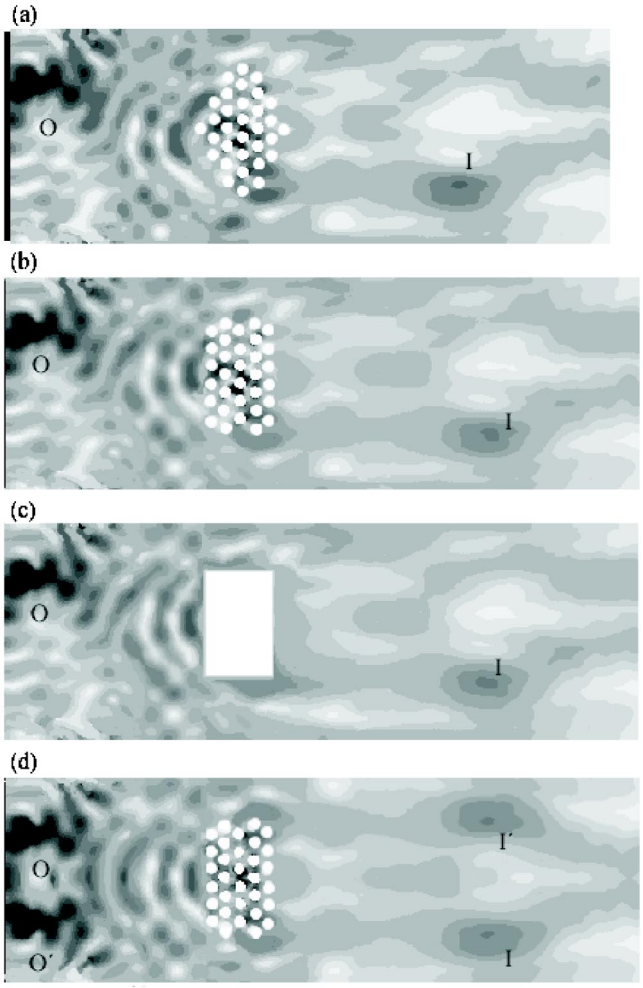

FIG. 2. (a) Imaging of a point source by a biconvex lens consisting of an array of Al cylinders. (b) Same pattern as in (a) with a rectangular lens. (c) Same pattern as in (a) with a rectangular piece of aluminum. (d) Image of a two-point source with the rectangular lens of (b).

coherent waves interfere and a clear two-point image appears behind the slab. The same effect (although not shown here) is obtained by placing two point sources in front of a massive aluminum block, like the one of Fig. 2(c). This proves unambiguously again the existence of an imaging mechanism based exclusively on diffraction effects, and constitutes a new result that introduces a broad spectrum of potential applications.

This diffractive influence of the device edge is illustrated by Babinet's principle, which relates the diffracted field built by complementary objects. This principle has been proven in optics following Kirchhoff's diffraction theory [11] and also applies to elastic waves [13]. Let two objects have complementary transmission functions q_1 and q_2, i.e., for uniform illumination: $q_1(x,y)+q_2(x,y)=1$. For opaque and transparent objects, respectively, this means that the opaque areas of the former are the transparent parts of the latter, and vice versa. Their corresponding diffracted fields angular spectra $Q_1(u,v)$ and $Q_2(u,v)$ are therefore related by $Q_2(u,v)=\delta(u)\delta(v)-Q_1(u,v)$, $\delta(u),\delta(v)$ being the δ functions,

and $Q_1(u,v)$ and $Q_2(u,v)$ standing for the Fourier transforms of $q_1(x,y)$ and $q_2(x,y)$, respectively; u and v denoting the corresponding spatial frequencies. The angular intensities $|Q_2(u,v)|^2$, $|Q_1(u,v)|^2$ of both complementary objects are equal except at the origin. This principle is illustrated in the near field intensity distributions (calculated from these angular spectra and represented in Fig. 1(c)] on comparing these distributions, both to the right, Q_1, and below, Q_2, the imaging aluminum block. Inner diffraction due to the anisotropic starlike shape of the isofrequency curves near the gap [7] can even play an important complementary role in the subtle imaging mechanism of this *plane lens* phenomenon.

Direct analytical calculation of both external edgelike and inner, periodically modulated, degenerate diffraction mechanisms seems to be a formidable task at this point. As already shown, however, the FDTD method allows us to study simulations of such an elusive nature, and to appropriately design future useful experiments.

The FDTD method allows us to observe direction changes of the wave front because the amplitude changes are observable in the same instant when they are generated. We next show a different phenomenon where the refraction effect dominates over diffractive ones. Accordingly, an acoustic refractive system can be designed in which, in contrast with the focusing process seen above, refraction now plays the main role. To unambiguously visualize a refractive effect based on a sonic crystal, we therefore present here the example of an acoustic prism able to change the propagation direction of a plane wave. The device is shaped by adequately truncating a square periodic arrangement of 42 aluminum cylinders in air. The lattice parameter is 6.35 cm and the cylinder radius is 2 cm. The refraction by the prism of an incident plane acoustic wave at a frequency of 1700 Hz is clearly shown in Fig. 3. The refracted wave is also planar with a deviation angle of about 11.5°. The averaged angle of the prism, moreover, is estimated at 53°. If we apply Snell's law twice at both sides of the prism, we calculate a refractive index value $n=1.21$. On the other hand, the FDTD method allows us to calculate the sound velocity inside the acoustic composite by computing the time lapse employed by the wave front peak to propagate a given distance. Hence, from this velocity we can alternatively calculate the corresponding value of the refractive index, which we obtain as $n=1.25$. The slight discrepancy between both estimated refractive indices is likely due to anisotropic inner diffraction effects of the weakly modulated structure.

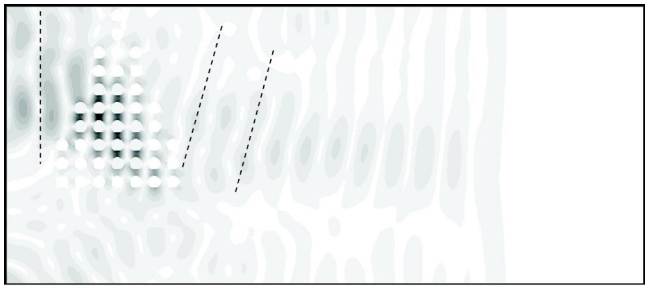

FIG. 3. Sound refracted, at 1700 Hz, by an acoustic prismlike structure, made with a square periodic array of aluminum rods. Diffraction does not preclude that the direction of the incident sound plane wave clearly changes by a deviation angle of about 11.5°.

In conclusion, composite acoustic devices with size dimensions of a few wavelengths are able to produce acoustic images. On the other hand, we show that the lens image formation in this size range is predominantly obtained through a diffraction mechanism rather than by refraction. Although intrinsically mixed, however, both diffractive and refractive properties can be exploited to control the change in the propagation direction of acoustic plane waves, as it has been illustrated here with a sonic prism. This ability can be useful in architectural acoustics, and for the design of ultrasonic solid devices. Finally, as a extreme consequence of the action of diffraction in image formation of acoustic, elastic, and optical waves, we have shown how a diffractive *massive block* certainly has lens properties. Indeed, our simulations indicate that diffraction plane lenses of the size of a few wavelengths are possible. This opens a new path for further research.

To close, it is interesting to mention that using the same FTDT method we have integrated the Maxwell's equations. The results [14] show that for electromagnetic radiation, the lensing also take place by diffraction when the lens is a few wavelengths in size as could be expected. In particular, the calculations have been done for a sphere and, to stress more the diffracting effect, by a biconcave lens that refraction should make it divergent.

This work has been supported by the DGICYT.

[1] M.M. Sigalas and E.N. Economou, J. Sound Vib. **158**, 377 (1992); Solid State Commun. **86**, 141 (1993); Europhys. Lett. **36**, 241 (1996); M.S. Kushwaha, P. Halevi, L. Dobrzynski, and B. Djafari-Rouhani, Phys. Rev. Lett. **71**, 2022 (1993); M.S. Kushwaha, P. Halevi, G. Martinez, L. Dobrzynski, and B. Djafari-Rouhani, Phys. Rev. B **49**, 2313 (1994); E.N. Economou and M.M. Sigalas, *ibid.* **48**, 13 434 (1993).

[2] W.M. Robertson and W.F. Rudy III, J. Acoust. Soc. Am. **104**, 694 (1998); F.R. Montero de Espinosa, E. Jiménez, and M. Torres, Phys. Rev. Lett. **80**, 1208 (1998); J.V. Sánchez-Pérez, D. Caballero, R. Martinez-Sala, C. Rubio, J. Sanchez-Dehesa, F. Meseguer, J. Llinares, and F. Galvez, *ibid.* **80**, 5325 (1998); J.O. Vasseur, P.A. Deymier, B. Chenni, B. Djafari-Rouhani, L. Dobrzynski, and D. Prevost, *ibid.* **86**, 3012 (2001).

[3] D. García-Pablos, M. Sigalas, F.R. Montero de Espinosa, M. Torres, M. Kafesaki, and N. Garcia, Phys. Rev. Lett. **84**, 4349 (2000).

[4] M. Torres, F.R. Montero de Espinosa, D. García-Pablos, and N. Garcia, Phys. Rev. Lett. **82**, 3054 (1999); S. Yang, J.H. Page, Z. Liu, M.L. Cowan, C.T. Chan, and P. Sheng, *ibid.* **88**, 104301 (2002).

[5] P. Halevi, A.A. Krokhin, and J. Arriaga, Phys. Rev. Lett. **82**,

719 (1999); Appl. Phys. Lett. **75**, 2725 (1999); N. Garcia, E. V. Ponizovskaya, and J. Q. Xiao, *ibid.* **80**, 1120 (2002).

[6] F. Cervera, L. Sanchis, J.V. Sanchez-Perez, R. Martinez-Sala, C. Rubio, and F. Meseguer, Phys. Rev. Lett. **88**, 23 902 (2002).

[7] H. Kosaka, A. Tomita, T. Kawashima, T. Sato, and S. Kawakami, Phys. Rev. B **62**, 1477 (2000).

[8] A. Taflove, *The Finite-Difference Time-Domain Method* (Artech House, Boston, 1998).

[9] I.E. Psarobas, N. Stefanou, and A. Modinos, Phys. Rev. B **62**, 278 (2000); Z. Liu, T. Chan, P. Sheng, A.L. Goertzen, and J.H. Page, *ibid.* **62**, 2446 (2000).

[10] M. Kafesaki, M.M. Sigalas, and N. García, Phys. Rev. Lett. **85**, 4044 (2000).

[11] M. Born and E. Wolf, *Principles of Optics* (Cambridge University Press, Cambridge, 1999).

[12] J. W. Goodman, *Introduction to Fourier Optics* (McGraw-Hill, New York, 1968).

[13] A.F. Gangi and B.B. Mohanty, J. Acoust. Soc. Am. **53**, 525 (1973).

[14] N. Garcia, M. Nieto-Vesperinas, E. V. Ponizovskaya, and M. Torres (unpublished).